Marine Pollution Bulletin 169 (2021) 112594

Contents lists available at ScienceDirect

Marine Pollution Bulletin

journal homepage: www.elsevier.com/locate/marpolbul

Detecting stranded macro-litter categories on drone orthophoto by a multi-class Neural Network

Luis Pinto [a], Umberto Andriolo [b,*], Gil Gonçalves [b,c]

[a] University of Coimbra, CMUC, Department of Mathematics, Coimbra, Portugal
[b] INESC Coimbra, Department of Electrical and Computer Engineering, Coimbra, Portugal
[c] University of Coimbra, Department of Mathematics, Coimbra, Portugal

ARTICLE INFO

Keywords:
Drone
Machine learning
Beach pollution
Remote sensing
Coastal monitoring

ABSTRACT

The use of Unmanned Aerial Systems (UAS, aka drones) images for mapping macro-litter in the environment have been exponentially increasing in the recent years. In this work, we developed a multi-class Neural Network (NN) to automatically identify stranded plastic litter categories on an UAS-derived orthophoto.

The best results were assessed for items that did not have substantial intra-class colour variability, such as octopus pots and fishing ropes (F-score = 61%, on average). Instead, performance was poor (37%) for plastic bottles and fragments, due to their changing intra-class colours. On average, the performance improved 24% when the binary detection (litter/non-litter, F-Score = 73%) was considered, however this approach did not discriminate the litter categories.

This work gives a new perspective for the automated litter detection on drone images, suggesting that colour-based approach can be used to improve the categorization of stranded litter on UAS orthophoto.

1. Introduction

Marine litter is defined as the set of items that have been deliberately discarded, unintentionally lost, or transported by winds and rivers, into the sea and stranded on coast (GESAMP, 2019). Nowadays, the amount of litter in coastal environments has become a global issue of major concern due to its significant potential impact on marine ecosystems, marine life and human health (e.g., Werner et al., 2016). Marine litter consists of various materials, such as metal, glass, rubber and paper, nonetheless plastic represents the largest proportion (up to 80%) (Galgani et al., 2015). Plastic production increased 43% over the last decade (Ritchie and Roser, 2018), and evidence suggests that plastic pollution will be a persistent global environmental issue in the near future (Adyel, 2020).

The use of Unmanned Aerial Systems (UAS) images for characterizing the abundance of marine litter on beaches (Andriolo et al., 2020b; Deidun et al., 2018; Gonçalves et al., 2020b; Hengstmann and Fischer, 2020; Martin et al., 2018; Merlino et al., 2020) and coastal dunes (Andriolo et al., 2020a, 2021), along with floating on river (Geraeds et al., 2019) and sea waters (Garcia-Garin et al., 2020b, 2020a; Topouzelis et al., 2019), have been exponentially increasing in the last years.

The identification and detection of marine litter on images can be performed by manual image screening (Andriolo et al., 2021a), nevertheless the automatization of the process would permit faster and standardized procedure, avoiding the subjectivity and tedium of the manual marking task. The main efforts dedicated to the automated detection of stranded marine litter on drone images focused on the binary (litter/non-litter) classification approach, feasible to describe the items abundance and identify hotspots. The detection performance, expressed in terms of F-score statistical measure, ranged between 49% and 75% depending on the different machine learning classifiers used for the aim, such as pixel-based random forest (RF, Gonçalves et al., 2020c; Martin et al., 2018), convolutional neural network (CNN, Duarte et al., 2020; Fallati et al., 2019), and object-based RF, k-nearest neighbors (KNN) and support-vector machines (SVM) (Gonçalves et al., 2020a).

The recognition of the marine litter categories is, however, fundamental to understand their origin, in order to implement proper mitigation measures (Galgani et al., 2013; Veiga et al., 2016). Hence, advances in the automated identification of the specific litter categories are required. The RF classifier based on histogram of oriented gradients

* Corresponding author at: Institute for Systems Engineering and Computers at Coimbra, University of Coimbra, Apartado 3008, EC Santa Cruz, 3001-501 Coimbra, Portugal.

E-mail addresses: luisp@mat.uc.pt (L. Pinto), uandriolo@mat.uc.pt (U. Andriolo), gil@mat.uc.pt (G. Gonçalves).

https://doi.org/10.1016/j.marpolbul.2021.112594
Received 18 November 2020; Received in revised form 19 May 2021; Accepted 31 May 2021
Available online 9 June 2021

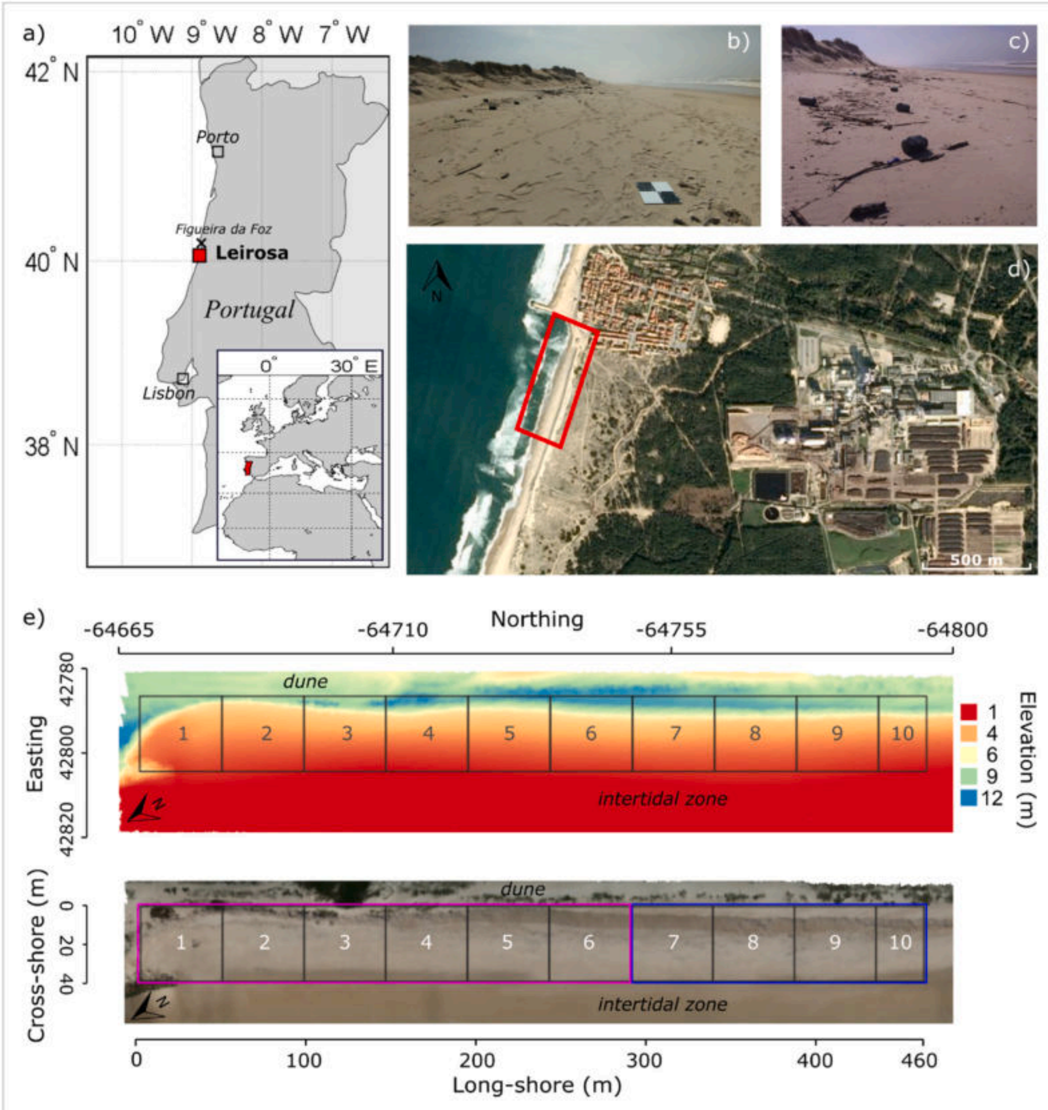

Fig. 1. Study site characterization. a) Study site location (red square); b–c) pictures taken prior the flight, with the drone take-off position (white-black target) and detail of marine litter on the beach, taken from the southern limit of the monitored area looking northward; d) study area (red rectangle) on satellite image; e) DSM (upper) and orthophoto (lower) produced from the UAS- image sequence, with sub-areas division (numbered rectangles from 1 to 10) for the application of machine learning algorithm. Magenta and blue frames indicate NN training and testing areas, respectively. (For interpretation of the references to colour in this figure legend, the reader is referred to the web version of this article.)

(HOG) features proposed by Martin et al. (2018) was shown to be not appropriate (F-score 14%), due to the high variability of litter items types, that can also be found with undefined shape (fragments), semi-buried, broken or crumpled (e.g., bottles). Therefore, it is of interest to investigate novel automated solutions that may allow to recognize the type of litter items on UAS-derived orthophoto.

This work developed a multi-class machine learning Neural Network for the automated identification of different stranded macro-litter items on drone images. We investigated the feasibility of a colour-based strategy for the distinction of litter categories, and compared the efficiency of the multi-class approach with the manual image screening and the binary (litter/non-litter) detections. For the aim, we used the orthophoto produced from a UAS flight over a beach-dune system on the North Atlantic Portuguese coast.

This work describes a new perspective to advance the automated categorization of marine litter on aerial images, for improving the use of UAS for marine litter mapping in the environment.

2. Methods

2.1. Study site and UAS data

A multirotor quadcopter DJI Phantom 4 RTK (DJI-P4RTK), equipped with a 20MP camera, was used to collect high-resolution images perpendicular to the direction of the flight on Leirosa beach (40°03′16.6″N 8°53′33.1″W), a sandy coastal stretch located on the North Atlantic coast of Portugal (Fig. 1) on 11 March 2020.

The drone flight altitude was set at 30 m above mean sea level (MSL), obtaining a ground sample distance (GSD) of 0.9 cm, suitable for the detection of marine macro-litter items (>2.5 cm, GESAMP, 2019). The orthophoto was produced with the Agisoft Metashape (v1.5.3) software, applying the Structure from Motion - MultiView Stereo (SfM-MVS) photogrammetric processing to the acquired image (5472 × 3648 pixels) block. The combination of flight altitude and battery autonomy allowed to cover an area extending 460 m long-shore and 120 m cross-shore (Fig. 1).

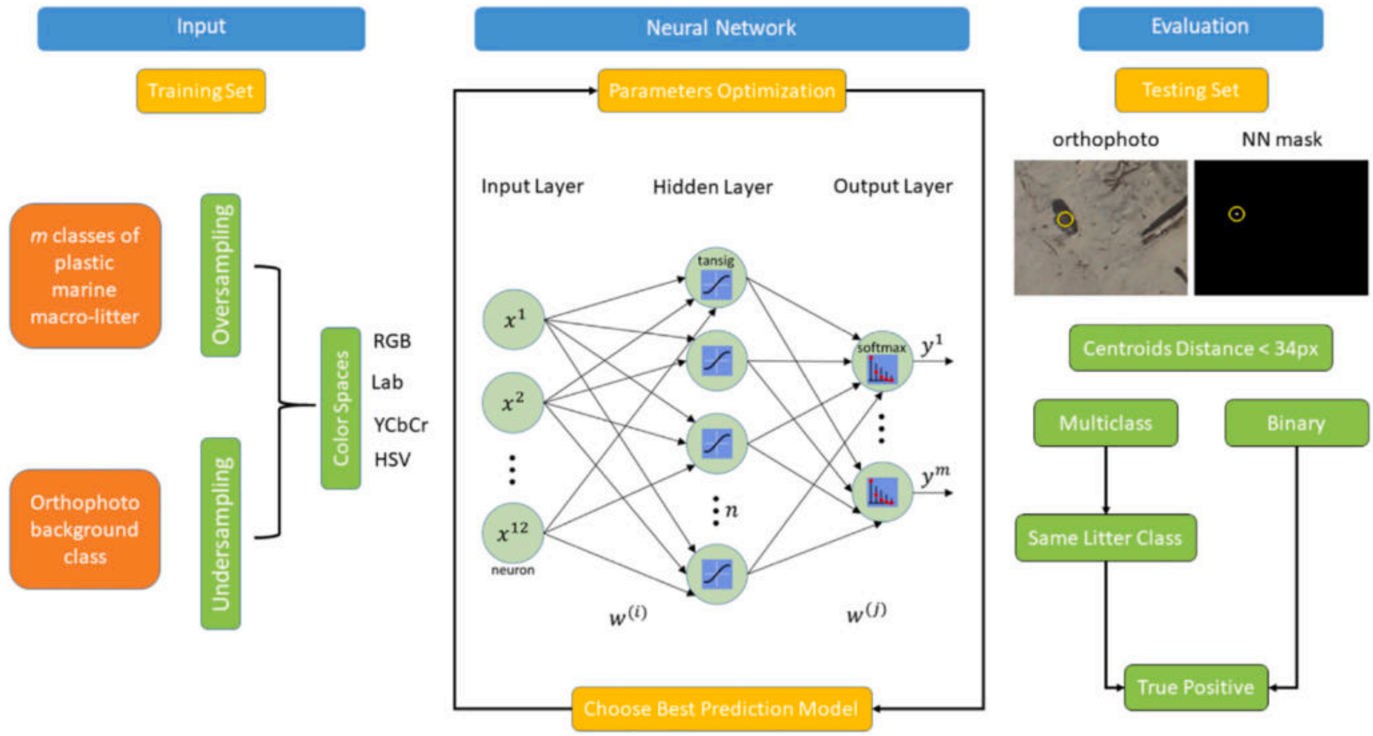

Fig. 2. Automated macro-litter detection workflow.

2.2. Manual image screening

The produced RGB orthophoto was first visually screened and manually processed by three operators in GIS environment, to mark the identified marine macro-litter items. In this work, we refer to this technique as manual image screening (hereinafter, MS).

The orthophoto was tiled with a 2 m × 2 m rectangular grid to make the MS procedure regular and organized. The operator marked each object recognized as marine litter in GIS environment, and tagged each item with the related OSPAR code number (OSPAR Commission, 2010) and its colour. The items with undefined shapes, which could not be related to specific categories, were labelled as “fragments”. The final outputs were i) the marine litter map and ii) the correspondent attribute table, with geolocation (longitude and latitude), category and colour of each item. An inter-observer reliability test was conducted among the MS of three operators to assess the consistency of the results.

2.3. The colour strategy

Stranded marine litter items can be recognized from their colours, as these much differ from the surrounding beach sand background. On the RGB orthophoto, each pixel had a red (R), green (G) and blue (B) value. However, in digital image processing, the conventional RGB colour space has been shown to be not perceptually uniform, as the colour spectrum values are highly correlated (Fairchild, 2013; Shaik et al., 2015). For this reason, previous works devoted to colour-based marine litter detection (Biermann et al., 2020; Gonçalves et al., 2020a, 2020c, 2020b; Kataoka et al., 2012; Kataoka and Nihei, 2020) have proposed the use of different colour models. In fact, the combination of more colour spaces has also been shown to be beneficial to improve image classification accuracy and to produce more robust classification systems. Following previous experiences (Gonçalves et al., 2020c, 2020b, 2020a), in this work we converted the RGB image values into three additional colour spaces, namely HSV, CIE-Lab and YCbCr. The HSV represents the colour spectrum in terms of hue (H), saturation (S) and brightness (V); in CIELab, the colour information is described by lightness (L) and two chromatic red-green (a) and blue-yellow (b) axis; in YCbCr, the luminance intensity (Y) is discriminated by the chrominance blue (Cb) and red (Cr) chrominance components (Fairchild, 2013).

2.4. Multi-class Neural Network

We adopted a multi-class approach for the automated detection of the distinct marine litter categories present on the beach (Fig. 2). For the aim, we developed a shallow feed-forward NN using the built-in algorithm available in Matlab environment. The NN is commonly trained with a set of chosen examples (training set) by a supervised learning algorithm, and then evaluated via a testing set. To simplify the application and to reduce the computational time of the NN, the orthophoto was divided into ten sub-areas, numbered progressively from 1 to 10 from north to south (Fig. 1). We considered the subareas 1–6 as training set (60%), while the 7–10 as testing set (40%). The sub-areas 1–9 (5332 × 4887 pixels) represented each about 40 m cross-shore and 50 m long-shore, while the sub-area 10 (3110 × 4887 pixel) measured 30 m long-shore.

Regarding the NN structure, this classifier is commonly composed by an input (first) layer, a hidden layer and an output (last) layer. Each layer has neurons that receive input from the previous layer and send the output to the next layer. The input layer consisted of twelve neurons corresponding to the size of the features vector, itself composed by the pixel intensity of the twelve colour channels (namely, R, G, B, H, S, V, L, a, b, Y, Cb, Cr) associated to each of the three values composing the colour spaces RGB, HSV, CIE-Lab, and YCbCr. The neurons in the NN are connected by weights (represented by w in Fig. 2) that are adjusted to minimize the error function during the training phase. In the task of marine litter classification, we aimed at minimizing the misfit between the predicted label for a given pixel and the true label of that pixel.

In the hidden layer, the common activation function (*tansig*, hyperbolic tangent sigmoid function) applies a nonlinear transformation to the input features and weights (Rawat and Wang, 2017). In terms of image classification, the identification of marine litter items on a high-

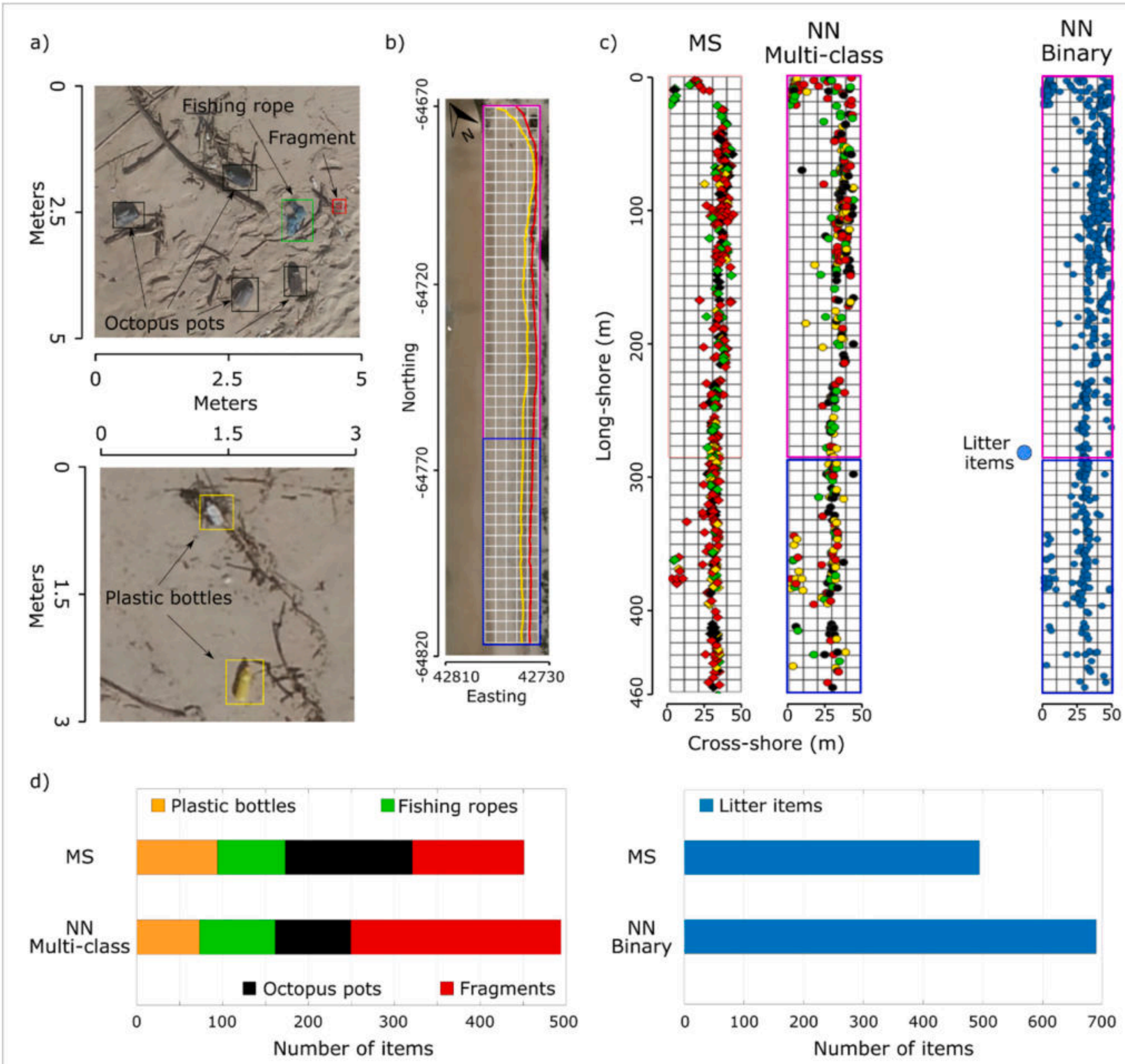

Fig. 3. Marine litter detection on Leirosa beach. a) Examples of the four types of items (rectangles) found on the beach and visible on the UAS-based orthophoto; b) beach orthophoto and grid (white rectangles) considered for the marking and mapping marine litter. Yellow and red lines indicate dune toe and dune crest, respectively; c) marine litter items marked on the grid by MS, NN multi-class and binary approaches. Common to c) and d), magenta and blue frames indicate NN training and testing areas, respectively. d) Histograms of the number of items marked by the different approaches on the monitored area. (For interpretation of the references to colour in this figure legend, the reader is referred to the web version of this article.)

resolution orthophoto (representing the beach surface) is a typical unbalanced classification problem (e.g., Duarte et al., 2020), as marine litter classes are represented by much less pixels than the image background. Thus, classification algorithms tend to overlook the minority classes (the *m* litter classes) in favour of the majority class (the non-litter class). To overcome this issue, we adopted undersampling and oversampling strategies to obtain a more balanced dataset where all classes were more evenly distributed.

The undersampling strategy aimed at reducing the number of samples of the majority class (non-litter), searching the areas of the images with homogeneous chroma background (sand). First, all sub-areas composing the training set were divided into regions of size 32 by 32 pixels (this size found by trial-and-error approach). Finally, we discarded most of the regions with homogeneous chroma and lowest standard deviation of pixel values. The oversampling strategy of the minority classes (marine litter items) improved the training set by adding synthetic items samples. We used the SMOTE (Synthetic Minority Oversampling Technique) function, which relies on the linear interpolation technique (Chawla et al., 2002).

To find the optimal number of neurons (n) in the hidden layer, the undersampling percentage and the oversampling percentage, we randomly divided the training sub-area set into two sub-sets, one for training (70% of sub-areas) and one for validation (30%). The optimal parameters combination was: 20 neurons in the hidden layer, 0.5% of

Table 1
Number and categories of marine litter found in Leirosa beach. The numbers and percentages of items composing the training and testing sets are also shown.

	Number of items	Percentage of marine litter	Training set		Testing set	
			N. of items	Percentage	N. of items	Percentage
Plastic bottles	70	14%	38	54%	32	46%
Fishing ropes	84	17%	65	77%	19	23%
Octopus pots	88	18%	57	65%	31	35%
Fragments	248	51%	167	67%	81	33%
Total	**490**		327	67%	163	33%

undersampling and 800% of oversampling.

The output layer consisted of $m + 1$ neurons, where m is the number of litter classes and $+1$ the non-litter class, and a suitable activation function (*softmax* function). Each neuron was associated with one of the $m + 1$ classes of our multi-class classification problem The output of each neuron was the probability of a given pixel belonging to the class associated with the respective neuron. These probabilities were used as input to an error function (cross-entropy) and the optimization algorithm used to train the NN was based on the scaled conjugate gradient algorithm.

For comparison purpose, we also adopted the binary approach for the NN application, considering only two classes: the litter class of marine litter items, in contrast with the non-litter class. The workflow followed the same procedure described for the multi-class approach (Fig. 2), whereas the structure of the NN was slightly modified. While in the multiclass approach there were $m + 1$ neurons in the output layer, one for the non-litter class and one for each one of the m litter classes, for the binary approach the output layer was composed by only of two neurons: one was associate to the litter class and the other to the non-litter class.

2.5. Performance evaluation

The automated detection performances were evaluated with the F-score statistical analysis, against the results obtained by the MS for the testing set (sub-areas 7–10, Fig. 1), for both multi-class and binary approaches.

The centroid of all the pixel regions labelled as marine litter items by the algorithms were compared to the centroids of marine litter items geotagged by the MS in the testing areas. For the multiclass approach, a true positive (TP) was registered when the distance between the items centroids was smaller than 34 pixels (30 cm, threshold), and the NN label was the same litter class than the MS label. If at least one of these two conditions was not satisfied, the detection was marked as false positive (FP). For the binary approach, only the geometrical condition of distance between centroids was considered. For both approaches, the 30 cm value was chosen as an appropriate threshold based on the average size of the macro-litter items (GESAMP, 2019). Finally, undetected marine litter items were counted as false negatives (FN). The new labels were used for the computation of the precision (P, detection relevance) as:

$$P = \frac{TP}{TP + FP} \tag{1}$$

the recall (R, detection rate), as:

$$R = \frac{TP}{TP + FN} \tag{2}$$

and the F-score (F, overall performance), which combines P and R as:

$$F = 2\frac{P\,R}{P + R} \tag{3}$$

All these indicators varied between 0 (worst result) and 100% (best classification).

Table 2
Statistical performance of NN multi-class approach in marine litter categories detection. True positive (TP), false negative (FN) and false positive (FP) detections were used to compute precision (P), recall (R) and the final F-score. In bold, the best values obtained for P, R and F-score.

	TP	FP	FN	P	R	F-score
Plastic bottles	11	22	21	33%	34%	34%
Fishing ropes	12	12	7	50%	63%	56%
Octopus pots	23	16	8	59%	**74%**	**66%**
Fragments	21	5	60	**81%**	26%	39%
Average				56%	49%	49%

3. Results

3.1. Manual image screening

Marine litter was mostly found at the upper beach profile (Fig. 3). Overall, 490 marine plastic litter items were identified and grouped into four main categories, namely plastic bottles, fishing ropes, octopus pots and plastic fragments (Table 1 and Fig. 3a).

Fragments represented 51% of the marine litter bulk, while each other category was found at similar rate (16% on average). Depending on items location in relation to the sub-areas 1–10 (Figs. 1e and 3), the NN training set was composed by the 67% of the litter items, and each category similarly represented (Table 1).

The inter-observer reliability test performed among the three operators did not return substantial differences in both marine litter detection and characterization.

3.2. Multi-class approach

Table 2 shows the NN performance in detecting the plastic items on the testing set. On average, the F-score was of 49%, nevertheless the assessment was different for each category. The octopus pots detection had the highest recall (R = 74%) and assessed the best results (F-score = 66%). Fishing ropes were detected with an F-score higher than 50%, whereas the worst results were for plastic bottles and fragments (37%, on average). The highest precision (P = 81%) obtained for the fragments category was determined by the low number of false positives (FP), nevertheless the lowest recall (R = 26%) indicated the highest number of missed items (Table 2 and Fig. 4d). On average, the F-score for the training set was of 47%, a close value to the F-Score (49%) obtained in the testing set, indicating that no overfitting occurred.

Fig. 4 shows the comparison between the maps produced by the manual and automated approaches. Regarding plastic bottles and octopus pots, automated detection returned FP in the northern sector, and overestimated plastic bottles at about 200 m long-shore location. Regarding the fragments category, the NN missed items mostly in the central and southern sectors of the beach, underestimating the items density. Nevertheless, the spatial distribution maps of the categories were similar, with all items distributed at the dune foot and all over the long-shore. The location of major concentrations (0.1 item m^{-2}) corresponded to the position of the hotspots obtained by the manual procedure (Fig. 4b). Some small differences were observed between the

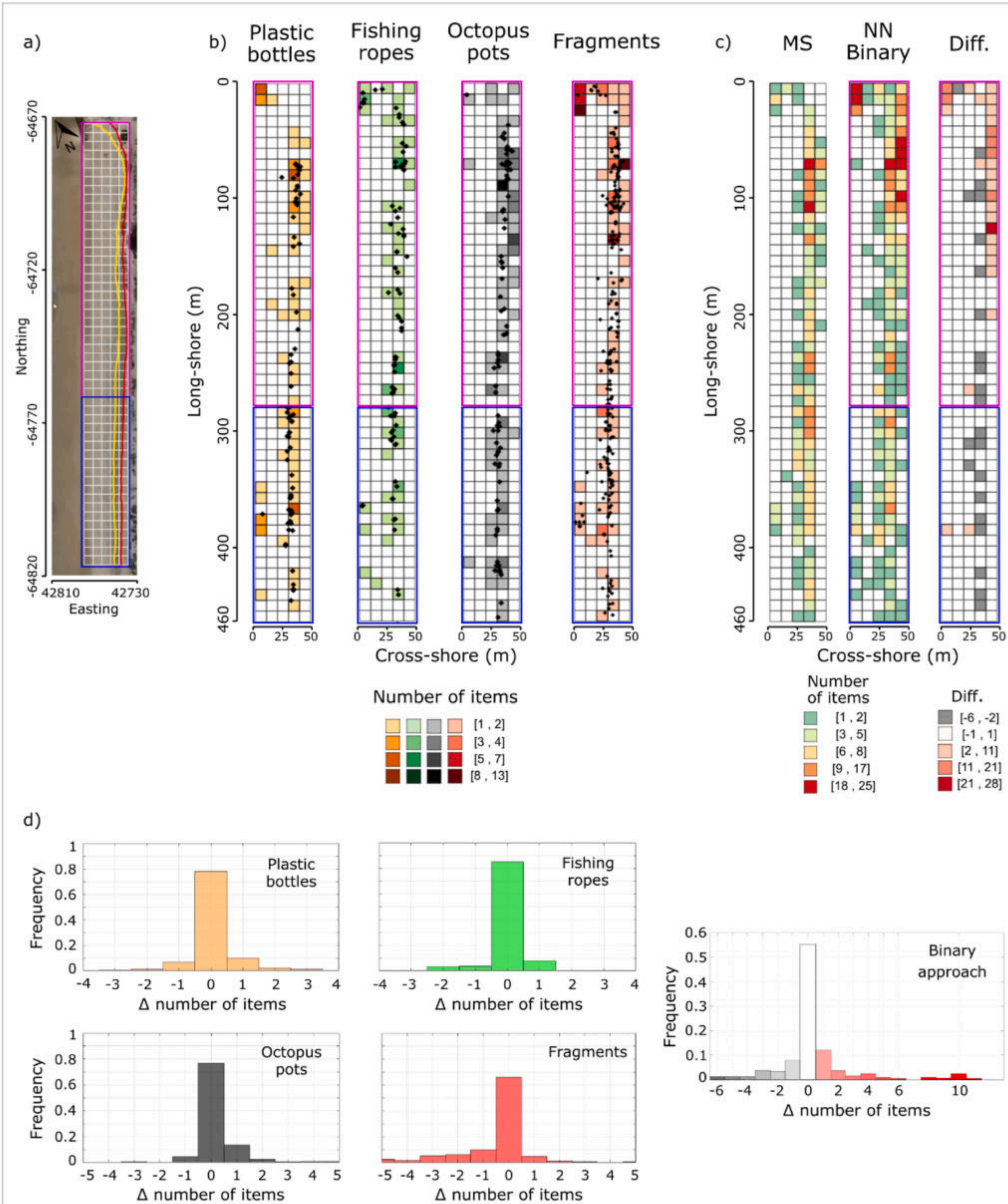

Fig. 4. Marine litter density maps. a) Beach orthophoto and grid (white rectangles) considered for marking and mapping marine litter. Yellow and red lines indicate dune toe and dune crest, respectively; b) density maps of marine litter categories produced by the multi-class Neural Network (NN) approach. Black dots indicate the items marked by the manual image screening (MS). Grid is formed by squares of 81 m^2; c) density maps of marine litter produced by MS (left), NN binary approach (middle) and difference between NN and MS (right). Common to a), b) and c), magenta and blue frames indicate NN training and testing areas, respectively. d) Histograms of the comparison among density maps produced from NN and MS. The histograms report the frequency of differences in the number of items within the 250 grid areas. (For interpretation of the references to colour in this figure legend, the reader is referred to the web version of this article.)

Table 3
Statistical performance of NN binary approach in marine litter detection, and average multi-class approach performance (see Table 2 for details). True positive (TP), false negative (FN) and false positive (FP) detections were used to compute Precision (P), recall (R) and the final F-score.

	TP	FP	FN	P	R	F-score
Binary	109	54	28	67%	80%	73%
Multi-class (average)	–	–	–	56%	49%	49%

locations of plastic bottles, which were not present at the northern sector of the beach, while the fishing ropes were found in smaller numbers in the southern limit of the monitored area. The map analysis also confirmed the best results obtained for octopus pots and fishing ropes, as the NN output described appropriately the abundance and distribution of these items.

In comparison with the multi-class approach, the binary strategy improved the average F-score of 24% (Table 3), with the limitation of indicating just the number of items and not the category (Fig. 3c). The abundance of marine litter was reasonably described, although both the white stones composing the groin head and the green dune vegetation were incorrectly recognized by the NN as marine litter in the northern sector of the beach (Fig. 4c–d).

4. Discussion

It has been shown how the use of UAS images allowed to detect and categorize the colour of marine litter items, which is also a relevant information for planning policy and mitigation measures (GESAMP, 2019). Hence, it has been proven the feasibility of a colour-based strategy to automatically identify and map the stranded plastic litter categories (Fig. 3) and their spatial distribution (Fig. 4). Despite the limited number of categories found and recognized on the UAS orthophoto at Leirosa beach (Table 1), the proposed colour features strategy may be a valuable alternative to deep learning architectures based on features inside their native structure (e.g., CNN). In fact, the colour information is less dependent on the drone flight altitude and consequently on the GSD, whereas other automated detection techniques may require lower flight altitude, hence higher image resolution, to assess a better classification (e.g., Fallati et al., 2019; Wolf et al., 2020). This is relevant for the UAS-based marine litter mapping, as the drone flight altitude determines the extent of the inspected area due to the limited drone battery autonomy.

The multi-class Neural Network (NN) machine learning algorithm returned the best results for those items that did not have intra-class colour variability (Table 4), namely octopus pots (97% were black, F-score = 66%) and fishing ropes (97% were green, F-score = 56%). On the contrary, the detection performances were lower for those items that presented high intra-class colour variance (plastic bottles and fragments). These last two categories also shared a large percentage of items with the same colour (white, 40% and 71% of plastic bottles and fragments, respectively), therefore the training process may also have been negatively affected by this factor. Nevertheless, the generated maps were fairly in agreement with the ones produced by the manual image

Table 4
Marine litter categories and related percentage of colour. In bold, the most signifcant percentages for each category.

	White (%)	Black (%)	Blue (%)	Red (%)	Green (%)	Yellow (%)	Brown (%)	Transparent (%)	F-score NN (%)	Number of items
Plastic bottles	**40**	1	1	3	8	1	1	**44**	34	70
Fishing ropes	–	–	–	3	**97**	–	–	–	56	84
Octopus pots	–	**96**	3	–	1	–	–	–	66	88
Fragments	**71**	8	5	9	3	4	–	1	39	248
Total	41	21	3	6	19	2	–	7		490

Table 5
Comparison of results obtained by published marine litter detection algorithms reporting i) machine learning method and approaches; ii) performance in term of precision (P), sensitivity (S) and F-score; iii) environment of application; iv) UAV flight altitude and GSD of the images used.

Reference	Method		Binary approach			Multi-class approach			Type of litter - environment	UAV flight altitude (GSD)
			P (%)	R (%)	F-score (%)	P (%)	R (%)	F-score (%)		
Martin et al., 2018	RF (Hog)	Pixel-based				8	35	13	Stranded litter - sandy beach	10 m (0.5 cm/pixels)
Fallati et al., 2019	CNN	Pixel-based	94 23[a]	67 25[a]	78 33[a]				Stranded litter - sandy beach	10 m (0.44 cm/pixels)
Gonçalves et al., 2020b	RF	Pixel-based	73	74	75				Stranded litter - sandy beach and dune	20 m (0.55 cm/pixel)
Gonçalves et al., 2020c	RF CNN	Pixel-based	70 55	71 65	70 60				Stranded litter - sandy beach and dune	20 m (0.55 cm/pixel)
Gonçalves et al., 2020a	RF SVM KNN	Object-based	75 76 68	68 62 62	72 68 65				Stranded litter - sandy beach and dune	20 m (0.55 cm/pixel)
Wolf et al., 2020	CNN	Pixel-based	75	72	73	55	83	67	Floating litter - water	6 m (0.2 cm/pixel)
Jakovljevic et al., 2020	ResUNet50	Pixel-based				72[b]	55[b]	60[b]	Floating litter – water	90 m (0.3 cm/pixel)
Garcia-Garin et al., 2021	CNN	Pixel-based	82	84	83				Floating litter – water	265 m (2.9 cm/pixel)
This work	Neural Network	Pixel-based	80	67	73	56	49	49	Stranded litter - sandy beach	30 m (0.9 cm/pixel)

[a] Obtained on images collected on a different beach from the trained dataset.

[b] Average values from Table 5 in Jakovljevic et al. (2020)).

screening (Fig. 4c), showing correctly the spatial distribution and the related hotspots of litter categories.

Results suggest that marine litter items with a low intra-class variability may be singularly targeted in future works. This represents an advance in comparison with the previous works proposing the automated litter items detection, as most of them considered the binary approach (Table 5). To our knowledge, the multi-class approach on UAS images has been adopted just to recognize floating litter categories and materials, returning better performances than in this work, however it is worth to note that water constitutes a different and more homogeneous background in comparison to sand (Jakovljevic et al., 2020; Wolf et al., 2020). As we implemented a pixel-based detection approach, future work may also investigate if the multi-class approach performance can be improved by the Object-based Image Analysis (OBIA, Gonçalves et al., 2020a), which allows to classify objects based on shape, texture and size, besides their spectral properties.

Several other authors have proposed different methods for the binary litter/not litter detection on aerial images (Bak et al., 2019; Bao et al., 2018; Kako et al., 2020; Kataoka et al., 2012; Kataoka and Nihei, 2020; Kylili et al., 2019; Panwar et al., 2020; van Lieshout et al., 2020), however the algorithms performances were not reported in terms of F-score, thus they were not included in the comparison shown in Table 5.

5. Conclusions

To improve the use of Unmanned Aerial Systems (UAS, aka drones) for marine litter mapping in the environment, we developed a multi-class Neural Network for the automated recognition of stranded litter categories on UAS images.

We tested the feasibility of a colour-based strategy for the recognition of stranded litter categories, which showed to be a viable solution to characterize the items on aerial images. Best performances were obtained for the marine litter categories that did not show inter-class colour variability (F-score = 62%, on average), whereas accuracy was poor for items with high variance of intra-class colours (37%). Overall, the detection performance improved 23% when the binary approach (litter/non-litter, F-Score = 73%) was considered. Therefore, the colour-based approach may support the selected detection of specific litter categories with chroma homogeneousness (in our case, octopus pots and fishing ropes). The binary approach was more appropriate for mapping the stranded litter abundance and identifying hotspots.

This work gives a new perspective for the automated detection of marine litter on drone images, suggesting that colour-based approach can be used to improve the categorization of stranded litter on UAS orthophoto.

CRediT authorship contribution statement

Luis Pinto: Conceptualization, Methodology, Formal Analysis, Data curation, Validation, Writing- Original draft preparation, Writing- Reviewing and Editing, Visualization.

Umberto Andriolo: Conceptualization, Methodology, Formal Analysis, Data curation, Validation, Writing- Original draft preparation, Writing – Review & Editing, Visualization,

Gil Gonçalves: Conceptualization, Methodology, Formal Analysis, Resources; Data curation, Writing- Reviewing and Editing, Supervision, Project Administration, Funding Acquisition

Declaration of competing interest

The authors declare that they have no known competing financial interests or personal relationships that could have appeared to influence the work reported in this paper.

Acknowledgments

This work was supported by the Portuguese Foundation for Science and Technology (FCT) and by the European Regional Development Fund (FEDER) through COMPETE 2020, Operational Program for Competitiveness and Internationalization (POCI) in the framework of UIDB/00308/2020 and the research project UAS4Litter (PTDC/EAM-REM/30324/2017). Luis Pinto was supported by the Centre for Mathematics of the University of Coimbra - UIDB/00324/2020, funded by the Portuguese Government through FCT/MCTES.

References

Adyel, T.M., 2020. Accumulation of plastic waste during COVID-19. Science. https://doi.org/10.1126/science.abd9925.

Andriolo, U., Gonçalves, G., Bessa, F., Sobral, P., 2020a. Mapping marine litter on coastal dunes with unmanned aerial systems: a showcase on the Atlantic Coast. Sci. Total Environ. 736. https://doi.org/10.1016/j.scitotenv.2020.139632.

Andriolo, U., Gonçalves, G., Sobral, P., Bessa, F., 2021. Spatial and size distribution of macro-litter on coastal dunes from drone images: a case study on the Atlantic coast. Mar. Pollut. Bull. 169, 112490. https://doi.org/10.1016/j.marpolbul.2021.112490.

Andriolo, U., Gonçalves, G., Rangel-Buitrago, N., Paterni, M., Bessa, F., Gonçalves, L., Sobral, P., Bini, M., Duarte, D., Fontán-Bouzas, A., Gonçalves, D., Kataoka, T., Luppichini, M., Pinto, L., Topouzelis, K., Vélez-Mendoza, A., Merlino, S., 2021a. Drones for litter mapping: An inter-operator concordance test in marking beached items on aerial images. Mar. Pollut. Bull. 169, 112542 https://doi.org/10.1016/j.marpolbul.2021.112542.

Andriolo, U., Gonçalves, G., Sobral, P., Fontán-Bouzas, Á., Bessa, F., 2020b. Beach-dune morphodynamics and marine macro-litter abundance: an integrated approach with unmanned aerial system. Sci. Total Environ. 749, 141474. https://doi.org/10.1016/j.scitotenv.2020.141474.

Bak, S.H., Hwang, D.H., Kim, H.M., Yoon, H.J., 2019. Detection and monitoring of beach litter using uav image and deep neural network. In: International Archives of the Photogrammetry, Remote Sensing and Spatial Information Sciences - ISPRS Archives, pp. 55–58. https://doi.org/10.5194/isprs-archives-XLII-3-W8-55-2019.

Bao, Z., Sha, J., Li, X., Hanchiso, T., Shifaw, E., 2018. Monitoring of beach litter by automatic interpretation of unmanned aerial vehicle images using the segmentation threshold method. Mar. Pollut. Bull. 137, 388–398. https://doi.org/10.1016/j.marpolbul.2018.08.009.

Biermann, L., Clewley, D., Martinez-Vicente, V., Topouzelis, K., 2020. Finding plastic patches in coastal waters using optical satellite data. Sci. Rep. https://doi.org/10.1038/s41598-020-62298-z.

Chawla, N.V., Bowyer, K.W., Hall, L.O., Kegelmeyer, W.P., 2002. SMOTE: synthetic minority over-sampling technique. J. Artif. Intell. Res. 16, 321–357. https://doi.org/10.1613/jair.953.

Deidun, A., Gauci, A., Lagorio, S., Galgani, F., 2018. Optimising beached litter monitoring protocols through aerial imagery. Mar. Pollut. Bull. 131, 212–217. https://doi.org/10.1016/j.marpolbul.2018.04.033.

Duarte, D., Andriolo, U., Gonçalves, G., 2020. Addressing the class imbalance problem in the automatic image classification of coastal litter from orthophotos derived from Uas imagery. In: ISPRS Ann. Photogramm. Remote Sens. Spat. Inf. Sci, V-3–2020, pp. 439–445. https://doi.org/10.5194/isprs-annals-v-3-2020-439-2020.

Fairchild, M.D., 2013. Color Appearance Models. John Wiley & Sons, Ltd, Chichester, UK. https://doi.org/10.1002/9781118653128.

Fallati, L., Polidori, A., Salvatore, C., Saponari, L., Savini, A., Galli, P., 2019. Anthropogenic marine debris assessment with unmanned aerial vehicle imagery and deep learning: a case study along the beaches of the Republic of Maldives. Sci. Total Environ. 693, 133581. https://doi.org/10.1016/j.scitotenv.2019.133581.

Galgani, F., Hanke, G., Werner, S., De Vrees, L., 2013. Marine litter within the European Marine Strategy Framework Directive. ICES J. Mar. Sci. 70, 1055–1064. https://doi.org/10.1093/icesjms/fst122.

Galgani, F., Hanke, G., Maes, T., 2015. Global distribution, composition and abundance of marine litter, in: Marine Anthropogenic Litter. https://doi.org/10.1007/978-3-319-16510-3_2.

Garcia-Garin, O., Aguilar, A., Borrell, A., Gozalbes, P., Lobo, A., Penadés-Suay, J., Raga, J.A., Revuelta, O., Serrano, M., Vighi, M., 2020a. Who's better at spotting? A comparison between aerial photography and observer-based methods to monitor floating marine litter and marine mega-fauna. Environ. Pollut. 258 https://doi.org/10.1016/j.envpol.2019.113680.

Garcia-Garin, O., Borrell, A., Aguilar, A., Cardona, L., Vighi, M., 2020b. Floating marine macro-litter in the North Western Mediterranean Sea: results from a combined monitoring approach. Mar. Pollut. Bull. https://doi.org/10.1016/j.marpolbul.2020.111467.

Garcia-Garin, O., Monleón-Getino, T., López-Brosa, P., Borrell, A., Aguilar, A., Borja-Robalino, R., Cardona, L., Vighi, M., 2021. Automatic detection and quantification of floating marine macro-litter in aerial images: introducing a novel deep learning approach connected to a web application in R. Environ. Pollut. https://doi.org/10.1016/j.envpol.2021.116490.

Geraeds, M., van Emmerik, T., de Vries, R., bin Ab Razak, M.S., 2019. Riverine plastic litter monitoring using Unmanned Aerial Vehicles (UAVs). Remote Sens. 11. doi: https://doi.org/10.3390/rs11172045.

GESAMP, 2019. Guidelines for the Monitoring and Assessment of Plastic Litter in the Ocean by Joint Group of Experts on the Scientific Aspects of Marine Environmental Protection, Gesamp (doi:ISSN: 1020-4873).

Gonçalves, G., Andriolo, U., Gonçalves, L., Sobral, P., Bessa, F., 2020a. Quantifying marine macro litter abundance on a sandy beach using unmanned aerial systems and object-oriented machine learning methods. Remote Sens. 12, 2599. https://doi.org/10.3390/rs12162599.

Gonçalves, G., Andriolo, U., Pinto, L., Bessa, F., 2020b. Mapping marine litter using UAS on a beach-dune system: a multidisciplinary approach. Sci. Total Environ. 706 https://doi.org/10.1016/j.scitotenv.2019.135742.

Gonçalves, G., Andriolo, U., Pinto, L., Duarte, D., 2020c. Mapping marine litter with unmanned aerial systems: a showcase comparison among manual image screening and machine learning techniques. Mar. Pollut. Bull. 155, 111158. https://doi.org/10.1016/j.marpolbul.2020.111158.

Hengstmann, E., Fischer, E.K., 2020. Anthropogenic litter in freshwater environments – study on lake beaches evaluating marine guidelines and aerial imaging. Environ. Res. 189 https://doi.org/10.1016/j.envres.2020.109945.

Jakovljevic, G., Govedarica, M., Alvarez-Taboada, F., 2020. A deep learning model for automatic plastic mapping using unmanned aerial vehicle (UAV) data. Remote Sens. 12 https://doi.org/10.3390/RS12091515.

Kako, S., Morita, S., Taneda, T., 2020. Estimation of plastic marine debris volumes on beaches using unmanned aerial vehicles and image processing based on deep learning. Mar. Pollut. Bull. 155 https://doi.org/10.1016/j.marpolbul.2020.111127.

Kataoka, T., Nihei, Y., 2020. Quantification of floating riverine macro-debris transport using an image processing approach. Sci. Rep. 10 https://doi.org/10.1038/s41598-020-59201-1.

Kataoka, T., Hinata, H., Kako, S., 2012. A new technique for detecting colored macro plastic debris on beaches using webcam images and CIELUV. Mar. Pollut. Bull. 64, 1829–1836. https://doi.org/10.1016/j.marpolbul.2012.06.006.

Kylili, K., Kyriakides, I., Artusi, A., Hadjistassou, C., 2019. Identifying floating plastic marine debris using a deep learning approach. Environ. Sci. Pollut. Res. 26, 17091–17099. https://doi.org/10.1007/s11356-019-05148-4.

Martin, C., Parkes, S., Zhang, Q., Zhang, X., McCabe, M.F., Duarte, C.M., 2018. Use of unmanned aerial vehicles for efficient beach litter monitoring. Mar. Pollut. Bull. 131, 662–673. https://doi.org/10.1016/j.marpolbul.2018.04.045.

Merlino, S., Paterni, M., Berton, A., Massetti, L., 2020. Unmanned aerial vehicles for debris survey in coastal areas: long-term monitoring programme to study spatial and temporal accumulation of the dynamics of beached marine litter. Remote Sens. 12, 1260. https://doi.org/10.3390/rs12081260.

OSPAR Commission, 2010. Guideline for Monitoring Marine Litter on the Beachs in the OSPAR Maritime Area (OSPAR Comm).

Panwar, H., Gupta, P.K., Siddiqui, M.K., Morales-Menendez, R., Bhardwaj, P., Sharma, S., Sarker, I.H., 2020. AquaVision: automating the detection of waste in water bodies using deep transfer learning. Case Stud. Chem. Environ. Eng. 100026 https://doi.org/10.1016/j.cscee.2020.100026.

Rawat, W., Wang, Z., 2017. Deep convolutional neural networks for image classification: a comprehensive review. Neural Comput. https://doi.org/10.1162/NECO_a_00990.

Ritchie, H., Roser, M., 2018. Plastic Pollution - Our World in Data [WWW Document]. OurWorldInData.org. https://ourworldindata.org/plastic-pollution#citation%0A. https://ourworldindata.org/plastic-pollution.

Shaik, K.B., Ganesan, P., Kalist, V., Sathish, B.S., Jenitha, J.M.M., 2015. Comparative study of skin color detection and segmentation in HSV and YCbCr color space. In: Procedia Computer Science, pp. 41–48. https://doi.org/10.1016/j.procs.2015.07.362.

Topouzelis, K., Papakonstantinou, A., Garaba, S.P., 2019. Detection of floating plastics from satellite and unmanned aerial systems (Plastic Litter Project 2018). Int. J. Appl. Earth Obs. Geoinf. 79, 175–183. https://doi.org/10.1016/j.jag.2019.03.011.

van Lieshout, C., van Oeveren, K., van Emmerik, T., Postma, E., 2020. Automated river plastic monitoring using deep learning and cameras. Earth Space Sci. 7. https://doi.org/10.1029/2019EA000960.

Veiga, J.M., Fleet, D., Kinsey, S., Nilsson, P., Vlachogianni, T., Werner, S., Galgani, F., Thompson, R.C., Dagevos, J., Gago, J., Sobral, P., Cronin, R., 2016. Identifying Sources of Marine Litter. MSFD GES TG Marine Litter Thematic Report, JRC Technical Reports. https://doi.org/10.2788/018068.

Werner, S., Budziak, A., Van Franeker, J.A., Galgani, F., Hanke, G., Maes, T., Matiddi, M., Nilsson, P., Oosterbaan, L., Priestland, E., Thompson, R., Veiga, J.M., Vlachogianni, T., 2016. Harm caused by Marine Litter - European Commission, JRC Scientific and Technical Reports. https://doi.org/10.2788/690366.

Wolf, M., van den Berg, K., Garaba, S.P., Gnann, N., Sattler, K., Stahl, F.T., Zielinski, O., 2020. Machine learning for aquatic plastic litter detection, classification and quantification (APLASTIC–Q). Environ. Res. Lett. https://doi.org/10.1088/1748-9326/abbd01.